Research Article

David I. Serrano-Garcia* and Yukitoshi Otani

Dynamic phase measurements based on a polarization Michelson interferometer employing a pixelated polarization camera

DOI 10.1515/aot-2016-0054
Received October 2, 2016; accepted November 14, 2016; previously published online December 28, 2016

Abstract: We implemented an interferometric configuration capable of following a phase variation in time. By using a pixelated polarization camera, the system is able to retrieve the phase information instantaneously avoiding the usage of moving components and the necessity of an extra replication method attached at the output of the interferometer. Taking into account the temporal stability obtained from the system, a spatial-temporal phase demodulation algorithm can be implemented on frequency domain for the dynamic phase measurement. Spatial resolution is analyzed experimentally using a USAF pattern, and dynamic phase measurements were done on air and water medium variations due to a jet flame and a living fish as a biological sample, respectively.

Keywords: interferometry; polarization camera; polarization phase-shifting technique; quantitative phase imaging.

1 Introduction

Optical measurement techniques have become indispensable tools in many areas of science and engineering. The contactless and highly accurate measurement capabilities are among the principal features of these techniques. These techniques encode the sample information in the phase of a two-dimensional (2-D) fringe pattern; several phase-shifted replicas of this fringe pattern are used to retrieve information about the sample. The main purpose of dynamic phase-shifting interferometry (DPSI) is to collect all the phase-shifted data in a single exposure in order to minimize time-varying environmental effects. As the data are collected instantaneously, external vibrations and turbulence are greatly reduced.

The use of phase shifting modulated by polarization has the advantage of not requiring mechanical components, such as a piezoelectric transducer (PZT), to obtain the phase shifts. A common optical system uses linear polarizing filters and quarter-wave plates to achieve modulation [1, 2]. Another property of a single-shot interferometer is the capability to obtain the necessary information to retrieve the phase information in a single capture. These systems are commonly based on replication methods like amplitude/phase gratings [3], adding extra components for getting replicas of the interferograms [4, 5], or using a pixelated polarizing camera [6, 7]. Each of these systems has its own properties that need to be taken into account at the moment of the phase demodulation process.

A pixelated polarizing camera presents the characteristic of having a special mask aligned with the CCD sensor. This mask is composed of a special pattern where a linear polarizer at different angles is associated within each pixel on the CCD sensor. By taking into account this intrinsic characteristic, phase demodulation algorithms [8–10] and interferometric systems [7, 11] have been proposed with the final purpose of retrieving the phase information of the sample in a single capture in a more focused manner.

Commercial systems can be encountered on the literature using similar techniques [12, 13]. For example, a microscopic dynamic interferometer was developed for biological purposes [7, 14–16]. The system uses a Linnik interference microscope employing a Kohler-type illumination. The authors tailored the temporal and spatial coherence property of the system using a diode laser system with spectral bandwidth of ~1.5 nm focused on a rotating

***Corresponding author: David I. Serrano-Garcia,** Center for Optical Research and Education (CORE), Utsunomiya University, Utsunomiya, Tochigi Pref., Japan,
e-mail: serrano_d@opt.utsunomiya-u.ac.jp.
http://orcid.org/0000-0002-5326-8874
Yukitoshi Otani: Center for Optical Research and Education (CORE), Utsunomiya University, Utsunomiya, Tochigi Pref., Japan; and Faculty of Optical Engineering, Utsunomiya University, Utsunomiya, Tochigi Pref., Japan

diffuser and then coupled into a multimode optical fiber of 1000 μm. In addition, a background filtering data processing was developed based on a low-order Zernike polynomial function on the measured phase [15, 16].

In our case, our implementation is not focused on a microscopic measurement, and by the combination of the commercial speckle reducer system (Optotune LSR-3005, Optotune, Dietikon, Switzerland) and the spatial filter, we were able to use a green laser beam at a wavelength of 532 nm (Photop DPGL-2100F, Photop, Shanghai, China). In addition, the phase demodulation algorithm is based on a 3-D Fourier transform that takes into account the temporal variation and the spatial carrier obtained by the pixelated polarizing camera directly.

The implemented systems combine polarization and speckle reduction techniques in order to provide a stable phase measurement in time allowing an extra filtering process on the phase demodulation algorithm. As a proof of implementation, the system was tested on moving samples showing the feasibility of the implementation. The paper is divided mainly into three parts: the experimental setup characteristics, temporal-spatial phase demodulation implementation, and experimental results.

2 Polarization Michelson interferometer using a pixelated polarizing camera

The implemented configuration is based on a polarization Michelson interferometer (PMI) using a pixelated polarizing camera in order to obtain the phase information in a single capture (Figure 1). Using a laser as a source at $\lambda = 532$ nm, linearly polarized light at 45° is divided by the polarizing beam splitter (PBS). On the object and reference arms of the PMI, linear polarization states are 0° and 90°, respectively. The back propagation interferogram was imaged on the CCD sensor by the imaging system and the first beam splitter (BS). A quarter-wave plate (QWP) at 45° was used to obtain circularly polarized beams in the opposite direction and later interfered by the pixelated camera. In order to fulfill the polarization phase-shifting condition, the back propagated interferogram is imaged by the first BS and the imaging system (L_1, L_2) on the CCD sensor. Because we are imaging directly on the CCD sensor, a speckle reduction system was implemented at the entrance of the interferometer. The speckle reducer is composed by an in-plane vibrating diffuser at 300 Hz provided by Optotune [17] placed on the frequency plane of a 4-f system. It is important to note that the speckle reduction part reduces the coherence length of the measurement, and the Michelson arrangement was aligned to work at zero path difference for have a high-contrast fringe pattern. A commercially available pixelated polarizing camera provided by Photonics Lattice (PI-100) (Photonics, Sendai City, Japan) was used [18]. The polarizing mask is based on photonic crystal arrangements having a working wavelength at 533 nm, and the polarizer array is composed of a superpixel of four orientations replicated across the CCD sensor. The pixelated polarizing camera employs a USB camera having a spatial resolution of 1024×1360 pixels with a pixel size of 6 μm and an acquisition rate of 10 fps. An advantage of this system is the reduction of moving parts. The only components that need to be aligned are the linear polarizer and the quarter wave plate at the output.

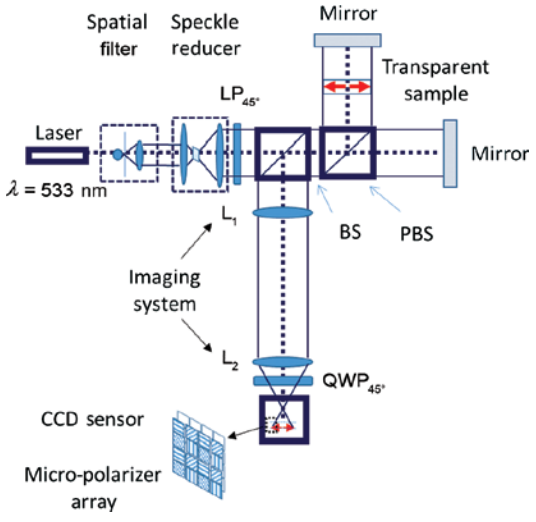

Figure 1: Polarization Michelson interferometer using a pixelated camera.

3 Spatial-temporal demodulation of phase dynamic measurement

Owing to the properties of the pixelated polarizing camera, a spatial distributed phase shift is introduced on the interferogram that can be taken into account for the phase demodulation process [8–11, 19]. The pixelated interferogram can be represented with a spatially distributed carrier, $pm(x,y)$, introduced by the pixelated polarizer mask aligned on the CCD sensor [10].

A common way of introducing a controllable spatial carrier on the interferograms is by using beam displacers or tilting a mirror in one of the arms of the interferometer [20]. In our case, we take into account the polarization properties of the pixelated camera, more exactly the

orientation variation of the polarizer array at each position. Because the implemented system is based on polarization phase-shifting techniques, the object and reference beams have circular polarization states in the opposite direction, and they are interfered by a polarizer at a specific orientation. The polarizer will introduce a controllable phase shift on the interferogram twice its orientation. Because the polarizer mask (placed on the CCD sensor) is composed by linear polarizers at known orientations and positions, the detected intensity by the pixelated camera could be seen as an interferogram with a known spatial dependence carrier used for demodulation.

The implemented system permits a stable acquisition in time presenting the advantage of introducing a filtering process on the temporal variation. The intensity detected by the CCD sensor can be represented as:

$$I(x,y,t) = A(x,y,t) + B(x,y,t)\mathrm{Cos}\left[\varphi(x,y,t) + pm(x,y)\right], \quad (1)$$

where $A(x,y,t)$ and $B(x,y,t)$ are the bias and amplitude modulation terms, and $\varphi(x,y,t)$ is the desired dynamic phase term. By a Fourier filtering process, the information corresponding to the phase and amplitude modulation can be retrieved as

$$\begin{aligned} C(x,y,t) &= \frac{1}{2}B(x,y,t)e^{i\varphi(x,y,t)} \\ &= F^{-1}\left\{F[I(x,y,t)e^{-ipm(x,y)}]H(\omega_x,\omega_y,\omega_t)\right\}, \end{aligned} \quad (2)$$

where $F[\cdot]$ represents the 3-D Fourier transform operation to retrieve the spatial and temporal response of the information to be low-pass filtered by $H(\omega_x,\omega_y,\omega_t)$. In our case, we used a Gaussian function with a controlled variable width. The process achieved by eqn. (2) retrieves the phase dynamic measurement in a single filtering step, and it can be conveniently applied on a real-time measurement by an analogous low-pass filtering process in a space domain. In addition, information from the amplitude modulation $B(x,y,t)$ can be used for system alignment purposes, masking, or unwrapping process.

3.1 Experimental results

In order to analyze the spatial resolution properties of the implementation, a USAF resolution test target was placed on the object arm of the interferometer (Figure 2). Two regions were selected on the measurement to show the minimum resolvable groups of the USAF pattern (Region I) and line profile analysis (Region II). By the demodulation algorithm implemented, an analysis on the amplitude modulation channel was done. Line profiles are provided by the Group 0 Element 1 corresponding to a line width of 500 μm giving an experimental pixel separation of 14 μm on the object plane. Information on the inner elements of groups 2 and 3 that was used for proper alignment of the imaging system in real time is provided.

Dynamic phase measurements were done on a high-temperature torch model PT-XT distributed by SOTO. The jet flame generated by the sample can reach temperatures ranging up to 1300°C [21]. The combustion generated by the jet flame changes the refractive index of the air that can be sensed by the implementation. The measurement corresponds to the change of the light passing through the jet flame combustion varying in time (Figure 3). It can be observed in Figure 3A that there is an inner profile distribution corresponding to the jet flame combustion and how the refractive index is changing surrounding it. The amplitude modulation term shows a specific distribution on the borders of the refractive changes giving information possibly on the beam deflection on this region. The

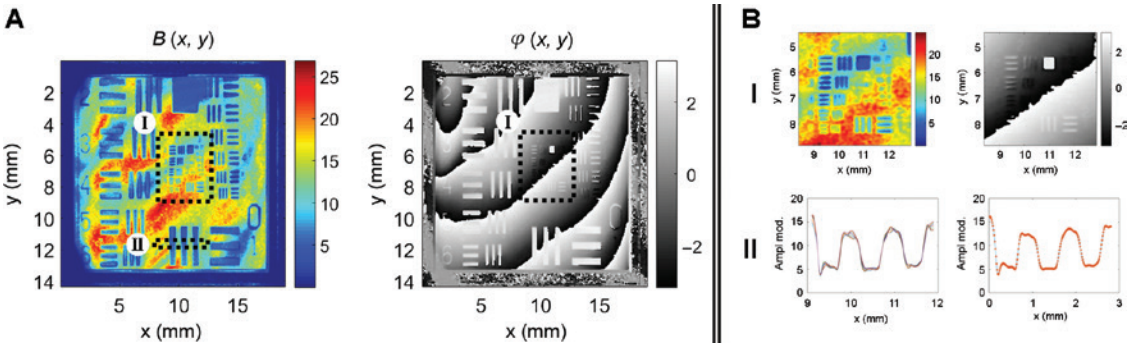

Figure 2: USAF Pattern as a sample for analyzing spatial resolution properties of the implementation. (A) The corresponding amplitude modulation and phase term and (B) two selected regions to analyze spatial properties of the measurement. Region I refers to the minimum resolvable groups, and Region II addresses the amplitude modulation variation on a selected profile giving an experimental pixel separation of 14 μm experimentally after a subpixel approach.

jet flame was followed by 37.2 seg corresponding to 372 frames shown in media 1, and Figure 3B shows four different frames on the measurement. Goldstein branch cut algorithm [22] was used for the unwrapped process.

By placing a container in each of the arm of the interferometer, for OPD matching conditions, a quantitative phase measurement can be done on the variation of the water as a medium caused by a living sample. In this case, we placed *Palaemonetes paludosus* commonly called ghost shrimp [23], and the system is capable of measuring the refractive index variation by the movement of the sample (Figure 4). Figure 4A shows the amplitude modulation and phase term of the measurement. It is worth mentioning that there is a static spatial distribution obtained due to the container used, and it was removed by taking the last frame as a reference. Temporal variations of amplitude modulation and wrapped phase are provided in media 2 and unwrapped phase in media 3.

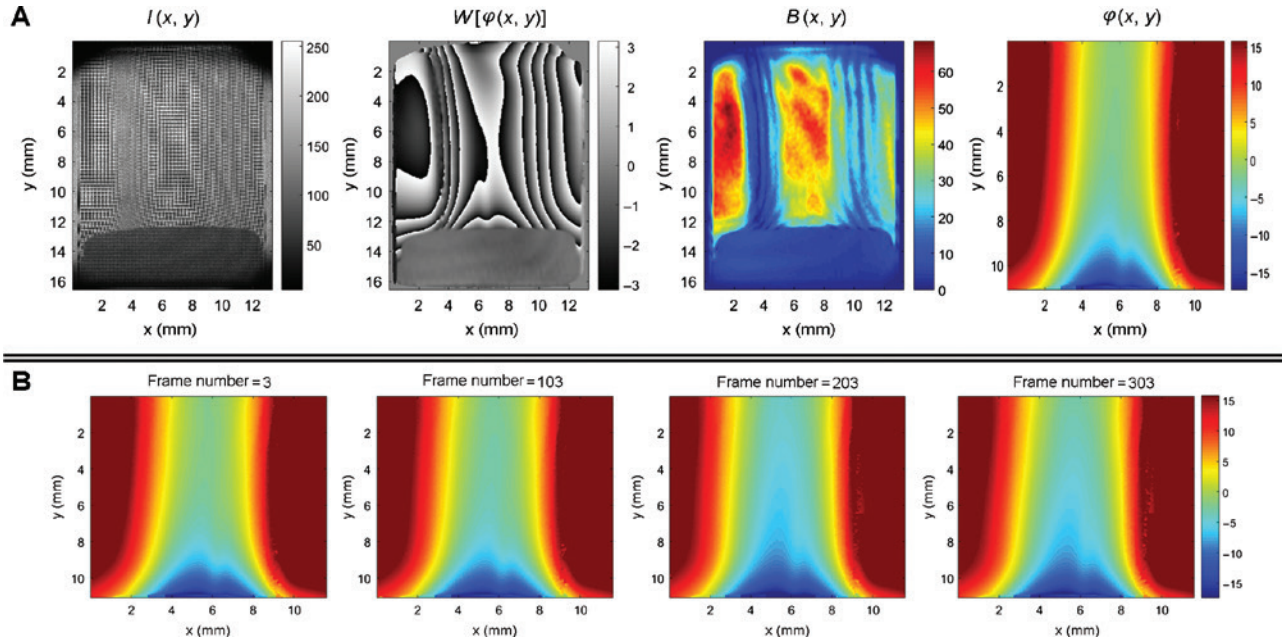

Figure 3: High-temperature torch varying in time was used as dynamic phase sample. (A) The corresponding pixelated interferogram, amplitude, and phase modulation term of a single frame and (B) characteristic frames of the temporal measurement shown in media 1.

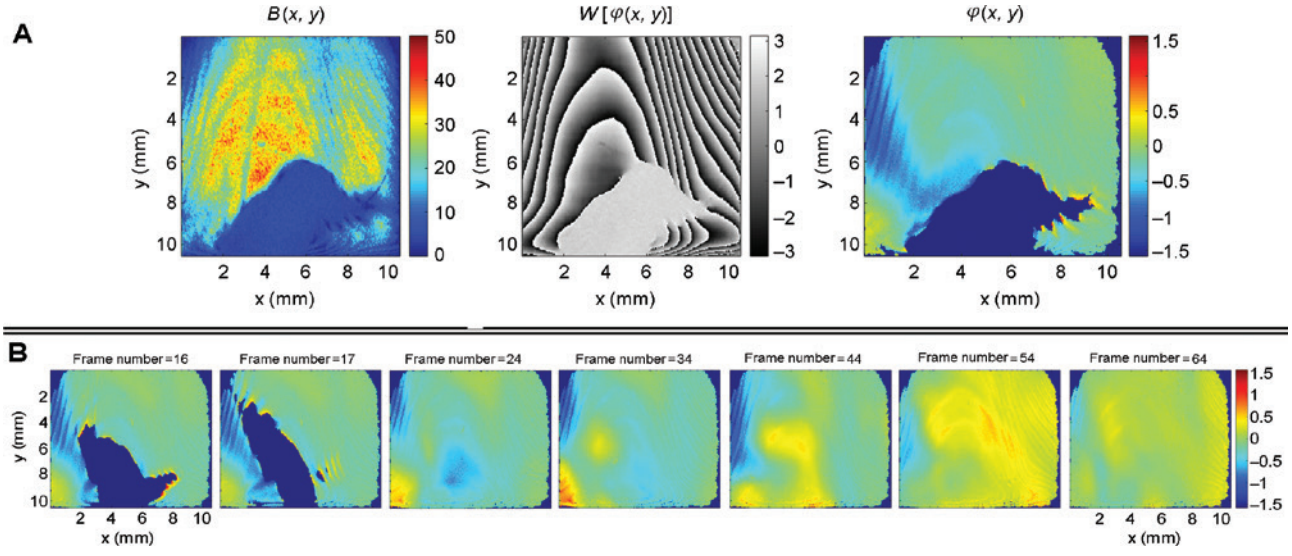

Figure 4: A living sample was placed on one of the arm of the interferometer, and medium variation can be observed due to its movement. (A) The corresponding amplitude and phase modulation term and (B) three frames of the temporal measurement shown in media 3.

4 Conclusions

By combining the interferometer, pixelated polarizing camera, phase demodulation algorithm, and speckle reduction system, the implementation itself shows the capability of following phase dynamic changes in a stable manner. Some of the limitations of the implementation can be encountered in the characteristics of the pixelated camera, fix number of elements on the mask, and imaging system selected. The phase variation was treated as a pure phase sample with no polarization changes. In the case of polarization variation, extra calibration procedures can be done in order to maintain the polarization phase-shifting conditions on the object and reference beam.

The system presents capabilities to be used in high-temperature condition samples and also by analyzing temporal variation occurring in living samples in another medium different from air.

Acknowledgments: The authors acknowledge the funding support provided under The Project for Bio-Imaging and Sensing at Utsunomiya University. D.I. Serrano-García is currently occupying a post doc position at Utsunomiya University in the Center for Optical Research and Education under the same project.

References

[1] P. Hariharan, Appl. Opt. 35, 6823–6824 (1996).
[2] S. S. Helen, M. P. Kothiyal and R. S. Sirohi, Opt. Commun. 154, 249–254 (1998).
[3] D. I. Serrano-García, A. Martínez-García, N.-I. Toto-Arellano and Y. Otani, Opt. Eng. 53, 112202 (2014).
[4] D.-I. Serrano-García, A. Martinez-García, N.-I. Toto-Arellano and Y. Otani, Adv. Opt. Technol. 3, 401–406 (2014).
[5] N.-I. Toto-Arellano, D.-I. Serrano-García and A. Martínez-García, Opt. Express 21, 31983–31989 (2013).
[6] J. E. Millerd, N. J. Brock, J. B. Hayes, M. B. North-Morris, M. Novak, et al., Proc. SPIE 5531, 304–314 (2004).
[7] K. Creath and G. Goldstein, Biomed. Opt. Express 3, 2866–2880 (2012).
[8] M. Servin and J. C. Estrada, Opt. Express 18, 18492–18497 (2010).
[9] B. Kimbrough and J. Millerd, Proc. SPIE 85706, 77900K (2010).
[10] J. M. Padilla, M. Servin and J. C. Estrada, Opt. Express 19, 19508 (2011).
[11] M. Novak, J. Millerd, N. Brock, M. North-Morris, J. Hayes, et al., Appl. Opt. 44, 6861 (2005).
[12] J. H. Neal Brock, J. Millerd and J. Wyant, U.S. patent US20050046865 A1 (2004).
[13] N. Brock, J. Hayes, B. Kimbrough, J. E. Millerd, M. North-Morris, et al., Nov. Opt. Syst. Des. Optim. VIII 5875, 58750F01–58750F10 (2005).
[14] K. Creath and G. Goldstein, in SPIE BiOS, Ed. By C. J. Cogswell, T. G. Brown, J.-A. Conchello and T. Wilson (International Society for Optics and Photonics, 2013), Vol. 8589, p. 85891A–85891A.
[15] K. Creath and G. Goldstein, in 'Conference Proceedings: Annual International Conference of the IEEE Engineering in Medicine and Biology Society. IEEE Engineering in Medicine and Biology Society. Annual Conference', (2012), Vol. 2012, pp. 3163–3166.
[16] G. Goldstein and K. Creath, in 'SPIE Optical Engineering + Applications', (2012), Vol. 8493, p. 84930N.
[17] Optotune, 'LSR application note', http://www.optotune.com/images/products/Optotuneapplication note LSR.pdf.
[18] 'Photonic Lattice', http://www.photonic-lattice.com/.
[19] B. T. Kimbrough, Appl. Opt. 45, 4554 (2006).
[20] M. Takeda, Ind. Metrol. 1, 79–99 (1990).
[21] SOTO, 'PT-XT Pocket Torch Extended', http://www.sotooutdoors.com/products/item/PT-XT.html.
[22] M. D. Pritt and D. C. Ghiglia, 'Two-Dimensional Phase Unwrapping: Theory, Algorithms, and Software' (Wiley, 1998).
[23] Chelsea Baranowski, 'Palaemonetes paludosus – Riverine grass shrimp', http://animaldiversity.org/accounts/Palaemonetes_paludosus/.

Supplemental Material: The online version of this article (DOI: 10.1515/aot-2016-0054) offers supplementary material, available to authorized users.